DMD Fast Forward. Published on May 7, 2021 as DOI: 10.1124/dmd.121.000361
This article has not been copyedited and formatted. The final version may differ from this version.

A new intestinal model for analysis of drug absorption and interactions considering physiological translocation of contents

Satoshi Asano, Aoi Yoshitomo, Shizuka Hozuki, Hiromi Sato, Yasuhiro Kazuki, and Akihiro Hisaka

Clinical Pharmacology and Pharmacometrics, Graduate School of Pharmaceutical Sciences, Chiba University, Chiba, Japan (S.A., A.Y., S.H., H.S., A.H.); DMPK Research Department, Teijin Pharma Limited, Tokyo, Japan (S.A.); Chromosome Engineering Research Center, Tottori University, Tottori, Japan (Y.K.); Division of Genome and Cellular Functions, Department of Molecular and Cellular Biology, School of Life Science, Faculty of Medicine, Tottori University, Tottori, Japan (Y.K.)

Manuscript number: DMD-AR-2021-000361

DMD Fast Forward. Published on May 7, 2021 as DOI: 10.1124/dmd.121.000361
This article has not been copyedited and formatted. The final version may differ from this version.

Running title page

Running title: Intestinal model considers physiological drug translocation

Corresponding author: Akihiro Hisaka, Clinical Pharmacology and Pharmacometrics, Graduate School of Pharmaceutical Sciences, Chiba University, Chiba, Japan

telephone: +81 432262880

e-mail: hisaka-u@chiba.jp

The number of text pages: 32

The number of tables: 1

The number of figures: 9

The number of references: 56

The number of words in Abstract: 234

The number of words in Introduction: 632

The number of words in Discussion: 1499

DMD Fast Forward. Published on May 7, 2021 as DOI: 10.1124/dmd.121.000361
This article has not been copyedited and formatted. The final version may differ from this version.

Abbreviations

ACAT: Advanced Compartmental Absorption and Transit, ADAM: Advanced Dissolution, Absorption and Metabolism, AIC: Akaike's information criterion, ATOM: Advanced translocation model, AUC: Area under the curve, BFGS: Broyden-Fletcher-Goldfarb-Shanno, CAT: Compartmental Absorption and Transit, C_{ent}: Drug concentration in the enterocytes, $C_{ent,u}$: Unbound drug concentration in the enterocytes, CL: Clearance, CL_{int}: Intrinsic clearance, C_{max}: Maximum plasma concentration, CYP: Cytochrome P450, CL_R: Renal clearance, DI: Drug interactions, DTPA: Diethylenetriaminepentaacetic acid, D: Dispersion number, f: Free fraction, F_A: Absorption ratio, F_G: Intestinal bioavailability, F_AF_G: Product of F_A and F_G, GI: Gastrointestinal, GITA: GI-transit absorption, H_{villi}: Height of villi, iPS: Induced pluripotent stem cells, K_i: Inhibitory constant, K_m: Michaelis constant, M: intestinal flow rate, ME: Microvilli expansion, Napp: Numeric Analysis Program for Pharmacokinetics, P_{app}: Apparent permeability, PBPK: Physiologically based pharmacokinetic, P-gp: P-glycoprotein, P: Permeability, PS: Permeability surface area product, Q: Blood flow rate, T_{ent}: Thickness of enterocyte, TLM: Translocation model, t_{max}: the time to reach C_{max}, V: Volume, VE: Villi expansion, V_{lum}: Volume of the intestinal lumen, V_{max}: Maximum rate

DMD Fast Forward. Published on May 7, 2021 as DOI: 10.1124/dmd.121.000361
This article has not been copyedited and formatted. The final version may differ from this version.

Abstract

Precise prediction of drug absorption is key to the success of new drug development and efficacious pharmacotherapy. In this study, we developed a new absorption model, the advanced translocation model (ATOM), by extending our previous model, the translocation model. ATOM reproduces the translocation of a substance in the intestinal lumen using a partial differential equation with variable dispersion and convection terms to describe natural flow and micro-mixing within the intestine, under not only fasted but also fed conditions. In comparison with ATOM, it was suggested that a conventional absorption model, advanced compartmental absorption and transit model, tends to underestimate micro-mixing in the upper intestine, and it is difficult to adequately describe movements under the fasted and fed conditions. ATOM explains the observed nonlinear absorption of midazolam successfully, with a minimal number of scaling factors. Furthermore, ATOM considers the apical and basolateral membrane permeabilities of enterocytes separately and assumes compartmentation of the lamina propria, including blood vessels, to consider intestinal blood flow appropriately. ATOM estimates changes in the intestinal availability caused by drug interaction associated with inhibition of CYP3A and P-gp in the intestine. Additionally, ATOM can estimate the drug absorption in the fed state considering delayed intestinal drug flow. Therefore,

DMD Fast Forward. Published on May 7, 2021 as DOI: 10.1124/dmd.121.000361
This article has not been copyedited and formatted. The final version may differ from this version.

ATOM is a useful tool for the analysis of local pharmacokinetics in the gastrointestinal tract, especially for the estimation of nonlinear drug absorption that may involve various interactions with intestinal contents or other drugs.

DMD Fast Forward. Published on May 7, 2021 as DOI: 10.1124/dmd.121.000361
This article has not been copyedited and formatted. The final version may differ from this version.

Significance Statement

The advanced translocation model (ATOM) was newly developed that precisely explains various movements of intestinal contents including the fasted and fed conditions which cannot be adequately described by the current physiological pharmacokinetic models.

DMD Fast Forward. Published on May 7, 2021 as DOI: 10.1124/dmd.121.000361
This article has not been copyedited and formatted. The final version may differ from this version.

Introduction

Oral formulations are commonly used in pharmacotherapy because they can deliver medicinal ingredients safely in the body and can be prescribed to outpatients (Homayun et al., 2019). However, drug absorption is seriously affected by many factors, such as disintegration of the formulation, the solubility and stability of the drug, ~~or~~ interactions with intestinal contents, active efflux by transporters, such as P-glycoprotein (P-gp) and metabolism by cytochrome P450 (CYP) 3A (Mayer et al., 1996; Lu et al., 2017). For analysis of intestinal drug absorption, various pharmacokinetic models, such as Compartmental Absorption and Transit (CAT) model (Yu and Amidon, 1999), Advanced Compartmental Absorption and Transit (ACAT) model (Agoram et al., 2001; Huang et al., 2009), Advanced Dissolution, Absorption, and Metabolism (ADAM) model (Jamei et al., 2009), segregated-flow model (Cong et al., 2000; Pang and Chow, 2012), Q_{Gut} model (Gertz et al., 2010), GI-transit absorption (GITA) model (Kimura and Higaki, 2002; Haruta et al., 2002), and translocation model (TLM) (Ando et al., 2015) have been reported. Of these, Q_{Gut} model is a simple model using the parameter Q_{Gut} and has provided adequate predictions of observed intestinal availability (F_G) values (Gertz et al., 2010); however, its application to nonlinear absorption has yet to be reported. Conversely, more advanced models, such as CAT,

DMD Fast Forward. Published on May 7, 2021 as DOI: 10.1124/dmd.121.000361
This article has not been copyedited and formatted. The final version may differ from this version.

ACAT or ADAM, explain the heterogeneity of the gastrointestinal tracts using multiple compartments. Each compartment possesses metabolism and transport clearances, enabling reasonable simulation of time- and location-dependent drug absorption. These models have succeeded in predicting gastrointestinal drug absorption, including non-linear pharmacokinetics (Takano et al., 2016; Bolger et al., 2009).

It is noteworthy that, for these sophisticated models, multiple scaling factors are required to fill the gaps between *in vitro* and *in vivo* data. For example, scaling factors such as for the absorption surface area in each intestinal site (Hendriksen et al., 2003), V_{max} and K_m of metabolic enzymes or transporters are applied to predictions (Takano et al., 2016). However, the function of the scaling factors would deviate from the concept of a physiologically based pharmacokinetic (PBPK) model when the movement of the drug to each section of the small intestine is not consistent with assumptions of the model.

This problem may lie with the structures of these models that explain the translocation of a drug in the lumen from upstream to downstream. Since translocation of a drug is explained via successive first-order kinetics in CAT, ACAT and ADAM, the degree of mixing is always increasing; thus, mixing tends to be underestimated upstream and overestimated downstream, leading to overestimation of drug

DMD Fast Forward. Published on May 7, 2021 as DOI: 10.1124/dmd.121.000361
This article has not been copyedited and formatted. The final version may differ from this version.

concentrations upstream. For substrate drugs of metabolic enzymes or transporters, drug concentrations need to be estimated accurately at each intestinal site to consider potential nonlinear pharmacokinetics. In addition, it is necessary to include the appropriate description of blood flow in the capillary in these models. To overcome this issue, the segregated-flow model has been proposed to consider divisions of blood flow into the mucosa and submucosa (Cong et al., 2000; Pang and Chow, 2012).

Previously, we developed a TLM to solve these problems (Ando et al., 2015). To minimize the calculation load, the TLM has only one compartment for absorption, but its properties of movement are time-dependent and arbitrary. However, it is theoretically difficult to accommodate for interactions with other drugs or various contents in the gastrointestinal tract. Therefore, in this study, we constructed an advanced translocation model (ATOM) that describes drug movements in the lumen by dispersion and convection terms while maintaining the features of TLM. Dispersion models based on partial differential equations have been used in the field of local pharmacokinetics to explain drug clearances (Roberts and Rowland, 1986) and extended to non-linear pharmacokinetics (Hisaka and Sugiyama, 1998). Hence, we analyzed drug movements in the gastrointestinal tract using a dispersion model in ATOM, and compared the results with those of CAT model.

DMD Fast Forward. Published on May 7, 2021 as DOI: 10.1124/dmd.121.000361
This article has not been copyedited and formatted. The final version may differ from this version.

Method

Construction of ATOM

The structure of ATOM and descriptions of the parameters are shown in Fig. 1 and Table 1, respectively. The source codes of ATOM used for the analysis were attached in the Supplemental text. The esophagus, stomach, caecum/colon, and portal vein were expressed as separate compartments. The intestinal lumen was expressed as one-dimensional dispersion model with a location-dependent dispersion number and time-dependent convection term. The movements of drugs, water, and intestinal contents were assumed to be the same in the lumen and thus substance independent since micro-mixing and convection occur due to intestinal motility. In addition to these tissues responsible for drug absorption, compartments for the portal vein and liver as well as central and peripheral blood pools for the whole body were assumed to simulate drug plasma concentration. Detailed physiological parameters, such as pH, P-gp and CYP3A expressions along intestine, and differential equations for tissues other than the small intestine are shown in the Supplemental text. Overall, the definition of ATOM is quite similar to TLM (Ando et al., 2015), other than the movements of intestinal contents, to achieve equivalent predictions of oral availability in the absence of

DMD Fast Forward. Published on May 7, 2021 as DOI: 10.1124/dmd.121.000361
This article has not been copyedited and formatted. The final version may differ from this version.

interaction. Partial differential equations related to luminal drug movements are shown in equations 1 and 2.

$$\frac{\partial C_{lum,z}}{\partial t} = D_z \frac{\partial^2 C_{lum,z}}{\partial z^2} - M_t \frac{\partial C_{lum,z}}{\partial z} - PS_{a,in,z} \frac{f_{lum} C_{lum,z}}{X_{water,z}+V_{lum,z}} + PS_{a,out,z} \frac{f_{ent} C_{ent,z}}{V_{lum,z}} \quad (z = (0,1)) \quad (1)$$

Boundary condition:

$$C_{lum,z} - \frac{D_z \partial C_{lum,z}}{M_t \partial z} = \frac{k_{sto} C_{sto} V_{sto} \partial t}{V_{lum,z}} \quad (z = 0)$$

$$\frac{\partial C_{lum,z}}{\partial z} = 0 \quad (z =1) \quad (2)$$

In these equations, length is expressed as a ratio of volume until the location to the full volume of the intestinal lumen (V_{lum}). $C_{lum,z}$ and $C_{ent,z}$ are drug concentrations in the lumen and enterocytes at location z (i.e., within a small interval around z, the same will be applied hereafter), respectively. D_z and M_t represent the dispersion constant at location z and flow rate in the lumen at time t, respectively. The units of D_z and M_t are T^{-1}, as the length is normalized in equation 1. The metrics $V_{lum,z}$ and $X_{water,z}$ represent the volume of the physical lumen and amount of inflating water (that may be drunk,

DMD Fast Forward. Published on May 7, 2021 as DOI: 10.1124/dmd.121.000361
This article has not been copyedited and formatted. The final version may differ from this version.

secreted, and absorbed) at location z, respectively. The effective volume in the lumen used for calculation of the drug concentration to know absorption is $V_{lum,z} + X_{water,z}$, but it was assumed that $X_{water,z}$ does not affect the micro-mixing and flow rate. The amount of inflating water in the gastrointestinal tract was simulated with a distinct partial differential equation by considering the water secretion and absorption rate constants calculated using intestinal water content after drinking 240 mL of water (Mudie et al., 2014). The simulation results of the water profile in the stomach and small intestine and the optimized parameter values are shown in Supplemental Fig. 1 and Table S1. $PS_{a,in,z}$ and $PS_{a,out,z}$ are the permeability clearance of the uptake from the lumen to the enterocytes and of the efflux from enterocytes to the lumen, respectively, via the apical membrane at location z. In this study, $PS_{a,out,z}$ is the sum of permeability clearance ($PS_{abs,api}$) and transport clearance by P-gp ($PS_{a,Pgp}$) shown in the Supplemental text. f_{lum} and f_{ent} represent drug unbound fractions in the lumen and enterocytes, respectively. In this study, f_{lum} and f_{ent} were assumed to be 1 and same as the unbound fraction in the blood (f_b) as described in Supplemental text, respectively. $V_{ent,z}$ is the volume of the enterocytes at location z.

Dispersion number and flow rate have been constant in general dispersion models for the analysis of local pharmacokinetics; however, drug distribution in the

DMD Fast Forward. Published on May 7, 2021 as DOI: 10.1124/dmd.121.000361
This article has not been copyedited and formatted. The final version may differ from this version.

small intestine is quite complicated because of its structural or regional differences in motility (Sokolis, 2012). Therefore, the location-dependent dispersion number (D_z) and time-dependent flow rate (M_t) were examined in this study. They were independently optimized using the observed intestinal distribution of a non-absorptive drug, ^{99m}Tc-diethylenetriaminepentaacetic acid (^{99m}Tc-DTPA) (Haruta et al., 2002) by nonlinear least-squares method. Equations 3 and 4 were used for the calculation of D_z and M_t in both fasted and fed states.

$$D_z = A \exp(-B\, z) + 0.005 \quad (3)$$

$$M_t = C\left(1 - D \exp\left(\frac{|t - t_{lag}|^F}{2E^F}\right)\right) \quad (4)$$

where A, B, C, D, E, and F are the adjusting constants, t is the time after administration, and t_{lag} is the time at the minimum flow rate. Parameters A-E and t_{lag} were optimized simultaneously using the observed ^{99m}Tc-DTPA distribution in the lumen reported by Haruta et al. (2002). The parameter F was fixed to 4 in this study. Among models that fixed for both D_Z and M_t, variable D_Z but fixed M_t, and variable D_Z and M_t, the best model was selected based on the Akaike's information criterion (AIC) value.

DMD Fast Forward. Published on May 7, 2021 as DOI: 10.1124/dmd.121.000361
This article has not been copyedited and formatted. The final version may differ from this version.

Regarding perpetrators of DI, drug concentrations of the perpetrator in tissues were simulated with partial differential equations in the intestine (equations 1-4) and differential equations in other tissues (shown in Supplemental text) as well as substrates. Intestinal clearance changes of P-gp transport and CYP3A metabolism upon administration of a perpetrator were calculated using equations 5 and 6 with unbound drug concentration of a perpetrator and inhibition constant for P-gp ($K_{i,Pgp}$) and CYP3A ($K_{i,CYP3A}$).

$$PS^{*}_{a,Pgp,z} = \frac{PS_{a,Pgp,z}}{1+\frac{f_{ent,I}I_{ent,z}}{K_{i,Pgp}}} \quad (5)$$

$$CL^{*}_{ent,z} = \frac{CL_{ent,z}}{1+\frac{f_{ent,I}I_{ent,z}}{K_{i,CYP3A}}} \quad (6)$$

where $PS_{a,Pgp,z}$ and $CL_{ent,z}$ represent active transport clearance of a substrate by P-gp and intestinal intrinsic clearance of a substrate by CYP3A, respectively, in the absence of a perpetrator (shown in Supplemental text). $PS_{a,Pgp,z}^{*}$ and $CL_{ent,z}^{*}$ represent $PS_{a,Pgp,z}$ and $CL_{ent,z}$ values in the presence of a perpetrator, respectively. $f_{ent,I}$ and $I_{ent,z}$ are the unbound fraction and concentration in the enterocytes of a perpetrator, respectively.

DMD Fast Forward. Published on May 7, 2021 as DOI: 10.1124/dmd.121.000361
This article has not been copyedited and formatted. The final version may differ from this version.

Analysis with CAT model

For comparison, CAT model with six intestinal compartments was constructed in this study (Fig. 1). The initial three compartments were for the upper intestine and the latter for the lower intestine. Transit times of the CAT model were optimized to fit the reported movements of ^{99m}Tc-DTPA in the lumen (Haruta et al., 2002); original and optimized transit times are shown in Supplemental Table S3. The length of the small intestine, radius of the inlet and outlet of the intestine, CYP3A and P-gp expression profile, and pH gradient were the same as those adopted in ATOM.

Simulation of drug concentrations in enterocytes and absorption to portal vein

Drug concentration in enterocytes and accumulation of the compound in the portal vein were simulated using ATOM and CAT after oral administration (t = 0 hr). To predict drug concentrations in enterocytes, three timepoints (t = 0.5, 2, and 6 hr) were selected to evaluate the drug concentrations and compare the two models. In this analysis, a compound with low permeability (non-CYP3A and -P-gp substrate) was selected to clearly understand the difference in absorption sites between the two models. The model compound has the same physiological and pharmacokinetic parameters as midazolam (molecular weight, pKa values, $K_{m,CYP3A}$, and unbound fraction), except for

DMD Fast Forward. Published on May 7, 2021 as DOI: 10.1124/dmd.121.000361
This article has not been copyedited and formatted. The final version may differ from this version.

the apparent permeability in Caco-2 cells ($P_{app,Caco-2}$) and $V_{max,CYP3A}$ that were set to 0.002 cm/h (approximately 1/50 compared with midazolam) and 0 μg /h pmol CYP3A, respectively. Regarding dispersion number and flow rate, optimized values using ^{99m}Tc-DTPA distribution of one subject (subject A) in the fasted state (shown in Fig. 2A and Supplemental Table S2) were used. Dose was set to 1 ng.

Prediction of non-linear absorption of midazolam and unbound concentration in enterocytes in both fasted and fed state

Dose-dependent absorption ratio (F_AF_G) and concentrations in enterocytes with regard to typical CYP3A substrate (midazolam) were simulated for 4 h after oral administration using ATOM and CAT. In simulations by ATOM, F_AF_G values of midazolam were predicted in the fasted and fed states with the optimized dispersion numbers and intestinal flow rates determined using the ^{99m}Tc-DTPA distribution of subject A (Haruta et al., 2002), as shown in Fig. 2. It was confirmed that intestinal absorption of midazolam was completed at 4 h after oral administration. F_AF_G values were calculated using the equation 7.

F_AF_G:

DMD Fast Forward. Published on May 7, 2021 as DOI: 10.1124/dmd.121.000361
This article has not been copyedited and formatted. The final version may differ from this version.

$$F_A F_G = \frac{X_{PV,cumulative}}{Dose} \quad (7)$$

where $X_{PV,cumulative}$ represents accumulated drug amount in the portal vein.

Reported $F_A F_G$ values were obtained from previous reports (Ando et al., 2015; Bornemann et al., 1985). Pharmacokinetic parameters of midazolam and physiological parameters used in these models are shown in Supplemental Tables S4 and S5. To predict unbound drug concentration in enterocytes ($C_{ent,u}$), simulated results at 0.16 h after administration, at which maximum concentration was observed, were utilized.

Comparison of F_G predicted values between ATOM and TLM

F_G prediction by ATOM was performed using the same dataset (Supplemental Table S6) utilized in the previous report of TLM (Ando et al., 2015), and F_G values between ATOM and TLM were compared. In the simulation by ATOM, simulation results at 4 h after oral administration are shown because intestinal absorption was completed. F_G was calculated from absorption ratio (F_A) and $F_A F_G$ using the following equations (equations 8-9).

DMD Fast Forward. Published on May 7, 2021 as DOI: 10.1124/dmd.121.000361
This article has not been copyedited and formatted. The final version may differ from this version.

F_A:

$$F_A = 1 - \frac{X_{colon}}{Dose} \quad (8)$$

F_G:

$$F_G = \frac{F_A F_G}{1 - \frac{X_{colon}}{Dose}} \quad (9)$$

where $X_{PV,cumulative}$ represent accumulated drug amount in the portal vein. In the prediction of F_G values, optimized values using ^{99m}Tc-DTPA distribution of subject A in the fasted state (shown in Fig. 2A and Supplemental Table S2) were used.

Simulation of DI mediated by CYP3A and P-gp using ATOM

Regarding CYP3A-mediated DI simulation, reported plasma concentrations of midazolam with itraconazole (a typical CYP3A inhibitor) were used (Templeton et al., 2010). Briefly, 0, 50, 200, and 400 mg itraconazole were administered (t = 0 h) 4 h before midazolam administration, and then 2 mg midazolam was administered (t = 4 h). Regarding P-gp-mediated DI simulation, reported plasma concentrations of digoxin with clarithromycin (a typical P-gp inhibitor) were used (Rengelshausen et al., 2003). Briefly, 250 mg clarithromycin was administered (t = 0 h) twice a day. Twenty-four

DMD Fast Forward. Published on May 7, 2021 as DOI: 10.1124/dmd.121.000361
This article has not been copyedited and formatted. The final version may differ from this version.

hours after the first administration of clarithromycin, 0.75 mg digoxin was administered (t = 24 h). The plasma concentrations of midazolam and digoxin were simulated for 24 h after oral administration of the substrate in the presence or absence of a perpetrator according to the reports by Templeton et al. (2010) or Rengelshausen et al. (2003). DI simulation was performed using optimized values using ^{99m}Tc-DTPA distribution of subject A in the fasted state (shown in Fig. 2A and Supplemental Table S2) were used. In this simulation, only the intestinal contribution to the DI was considered, and thus, hepatic and renal inhibitions of the metabolizing enzyme or transporter were not included. The pharmacokinetic parameters of these drugs and the physiological values used in these analyses were obtained from previous reports or results using ADMET Predictor® and GastroPlus® (Simulations Plus, Inc.) shown in Supplemental Tables S4 and S5. Two pharmacokinetic parameters (f_p for digoxin and $K_{i,Pgp}$ for clarithromycin) were obtained from the printed labeling of Digoxin Elixir (Roxane Laboratories, Inc., available online: https://www.accessdata.fda.gov/drugsatfda_docs/nda/2004/021648s000_PRNTLBL.pdf) and the pharmacology reviews of PRADAXA (dabigatran etexilate mesylate) Capsules (Boehringer Ingelheim Pharmaceuticals, Inc., Available online: https://www.accessdata.fda.gov/drugsatfda_docs/nda/2010/022512Orig1s000PharmR_

DMD Fast Forward. Published on May 7, 2021 as DOI: 10.1124/dmd.121.000361
This article has not been copyedited and formatted. The final version may differ from this version.

Corrrected%203.11.2011.pdf), respectively. Body weight was assumed to be 70 kg for calculating pharmacokinetics parameters.

Simulation of plasma concentration after oral administration of midazolam and digoxin in the fasted and fed state

Plasma concentration of midazolam and digoxin in the fasted and fed state were simulated for 24 h after oral administration. Dose was set to 2 mg (midazolam) and 0.75 mg (digoxin), respectively. In these simulations, the dispersion constant and flow rate in the intestine obtained using ^{99m}Tc-DTPA distribution of subject A in fasted and fed state were used. The pharmacokinetic parameters of these drugs and the physiological values used in these analyses were obtained from previous reports or results using ADMET Predictor® and GastroPlus® (Simulations Plus, Inc.) shown in Supplemental Tables S4 and S5. Body weight was assumed to be 70 kg for calculating pharmacokinetics parameters.

Calculation of dispersion model

The model with three nonlinear partial differential schemes (substrate, perpetrator, and inflating water) was solved by FDM (Hisaka and Sugiyama, 1998),

DMD Fast Forward. Published on May 7, 2021 as DOI: 10.1124/dmd.121.000361
This article has not been copyedited and formatted. The final version may differ from this version.

with differential schemes for the associated organs (esophagus, stomach, colon, portal vein, liver, central and peripheral compartments of the body). The number of segments was determined to be 40 considering the precision of the calculation. The Danckwerts' (closed) boundary conditions were implemented. Schemes for all the segments and compartments were calculated simultaneously with the Runge-Kutta-Fehlberg method using Numeric Analysis Program for Pharmacokinetics, Napp (version 2.31) (Hisaka and Sugiyama, 1998). The parameter fitting was performed mainly by the quasi-Newton method with the Broyden–Fletcher–Goldfarb–Shanno (BFGS) scheme implemented in Napp.

DMD Fast Forward. Published on May 7, 2021 as DOI: 10.1124/dmd.121.000361
This article has not been copyedited and formatted. The final version may differ from this version.

Results

Determination of dispersion number in ATOM and application to the simulation of ^{99m}Tc-DTPA distribution in the lumen considering effect of food

ATOM explains movements of intestinal contents, including the target drug, by the dispersion model with potentially variable dispersion number and flow rate. Thus, these terms need to be determined to reproduce the observed movements of intestinal contents. In the fasted state, non-absorbable ^{99m}Tc-DTPA filled the upper jejunum within 2 h after dosing, and thereafter rapidly moved to the lower jejunum, where it was retained for the next 2 h according to the report by Haruta et al. (2002) (Fig. 2A, C, E, G). In the fed state, in addition to delayed gastric emptying, movement of the contents slowed and a part of it was retained in the upper jejunum even 3 h after dosing (Fig. 2B, D, F, H). The model with a location-dependent variable dispersion number successfully reproduced the movements of the rapid passage through the upper jejunum and the subsequent retention in the lower jejunum, but only for one of the two fasted subjects (Fig. 2A and 3A). The model with a fixed dispersion term failed to reproduce the movement even for this subject (Supplemental Fig. 2). For the remaining observations, including in the fed state, a model with time-dependent flow rate, in addition to the

DMD Fast Forward. Published on May 7, 2021 as DOI: 10.1124/dmd.121.000361
This article has not been copyedited and formatted. The final version may differ from this version.

location-dependent dispersion number, was necessary to explain the observed movements of radioactivity in the intestine (Fig. 2B, 2D and Fig. 3).

Simulated luminal distribution of ^{99m}Tc-DTPA by CAT model

The CAT model explains movements of intestinal contents with a set of transit times from one compartment to the next. A model with reported transit times (Heikkinen et al., 2012) failed to reproduce the observed movements of ^{99m}Tc-DTPA (Supplemental Fig. 3). Radioactivity was overestimated in the upper jejunum and underestimated in the lower jejunum in this model. Therefore, appropriate values of transit time were explored through a fitting analysis. Nevertheless, the distribution of ^{99m}Tc-DTPA was not reproduced in the CAT model, especially for within the lower jejunum and ileum in both fasted and fed states (Fig. 2E, F, G, H). The radioactivity flowed out to the large intestine early within 2 h, in all simulations using CAT.

Typical difference of estimated absorption site in ATOM and CAT model

Drug distribution in enterocytes is strongly affected by differences in concentrations in the lumen because a drug moves rapidly from the lumen to enterocytes. Therefore, we compared simulated drug concentrations in the enterocytes

DMD Fast Forward. Published on May 7, 2021 as DOI: 10.1124/dmd.121.000361
This article has not been copyedited and formatted. The final version may differ from this version.

using ATOM (using variable D_z and fixed M_t) and CAT (Fig. 4), in which parameters were optimized to explain the observed intestinal movements of ^{99m}Tc-DTPA. In this simulation, a drug with a low permeability (approximately 1/50 compared with midazolam) was used to explain a typical difference between the two models because notable differences in drug absorption between the two models are not observed for highly permeable drugs that are absorbed rapidly from the upper jejunum. The CAT model predicted higher drug concentrations in the upper jejunum at 0.5 and 2 h, but the drug was already considerably transferred from the lower jejunum to the ileum at 6 h. In contrast, ATOM predicted that the drug began to move to the lower jejunum even at 0.5 h and was retained there for 6 h. The cumulative drug amount reaching the portal vein from each section of the intestine was calculated for these conditions (Fig. 5). These results indicated that most of the drug was absorbed in the upper jejunum in the CAT model, while the absorption occurred mainly in the lower jejunum in ATOM.

Predicting non-linear absorption ratio of midazolam and confirmation of difference in CYP3A saturation in enterocytes between ATOM and CAT model

Intestinal metabolizing enzymes and transporters are saturated when drug concentrations are higher than the Michaelis constant (K_m) in the enterocytes during the

DMD Fast Forward. Published on May 7, 2021 as DOI: 10.1124/dmd.121.000361
This article has not been copyedited and formatted. The final version may differ from this version.

absorption process. Therefore, nonlinear dose responses of midazolam F_AF_G were simulated using the ATOM and CAT model in order to examine how drug movements in the intestinal lumen may affect oral bioavailability. When simulating results in the fasted state, F_AF_G after a midazolam dose of 0.1 mg were estimated as very similar in both the ATOM and CAT model. The value increased slightly at 1 mg in the CAT model; however, it remained consistent in ATOM (Fig. 6A). At 10 mg, the difference between the F_AF_G values estimated by the two models was most evident; the observed dose-response of F_AF_G for midazolam was more similar to the estimation by ATOM than that of the CAT model. Estimated unbound drug concentrations in the enterocytes at 0.16 h after dosing with 10 mg were compared between the ATOM and CAT model (Fig. 6B). In the CAT model, a higher peak unbound concentration was estimated (14.36 μg/mL) compared to that in ATOM (4.53 μg/mL). Therefore, the absorption window would be narrower in CAT than in ATOM. Since $K_{m,CYP3A,u}$ for midazolam is 1.08 μg/mL (Ando et al., 2015), the degree of saturation would be considerably more extensive in CAT than in ATOM. Additionally, F_AF_G values of midazolam were estimated to be lower in the fed state than in the fasted state by ATOM (Fig. 6A) because of the lower unbound concentration in the enterocytes in the fed state (Fig. 6B).

DMD Fast Forward. Published on May 7, 2021 as DOI: 10.1124/dmd.121.000361
This article has not been copyedited and formatted. The final version may differ from this version.

These results suggest that weaker and more realistic non-linear pharmacokinetics of drugs may be estimated by ATOM compared with CAT.

Consistency of F_G values predicted by ATOM and TLM

ATOM is an extended model of TLM that maintains various assumptions based on intestinal structures and absorption processes. A previous report by Ando et al. (2015) showed adequate correlation between predicted and calculated F_G values. Therefore, the F_G values predicted using ATOM and TLM were compared to confirm the consistency of the two models. As a result, F_G values predicted using ATOM were within 10% of those predicted using TLM (Fig. 7) for all the drugs examined (Supplemental Table S6). Hence, the results showed the consistency of ATOM and TLM.

Simulation of CYP3A or P-gp-mediated DIs using ATOM

ATOM is an expanded model from TLM, but TLM cannot simulate location-dependent DIs because it considers only one absorption site. Clinically, since CYP3A and P-gp are greatly involved in gastrointestinal absorption and many associated clinical DIs have been reported (Galetin et al., 2010; Kharasch et al., 2004;

DMD Fast Forward. Published on May 7, 2021 as DOI: 10.1124/dmd.121.000361
This article has not been copyedited and formatted. The final version may differ from this version.

Chu et al., 2018), it is important to be able to accurately predict DIs caused by them. Therefore, we selected midazolam as a typical substrate of CYP3A and digoxin as a typical substrate of P-gp, and we confirmed whether ATOM could explain DIs in combination with the typical perpetrators of CYP3A and P-gp, itraconazole and clarithromycin. The simulated profiles of the inhibitors were shown in Supplemental Fig. 6. Overall, increases in the plasma concentrations of midazolam and digoxin were simulated using ATOM when perpetrators were administered considering only the intestinal contribution (Fig. 8). However, the increase in midazolam concentrations tended to be overestimated for the 50 mg dose of itraconazole even though the contribution of the liver was not considered. On the other hand, in the higher doses, the elimination phase of midazolam was somewhat underestimated probably due to ignoring the hepatic contribution. Increases in F_A values of digoxin or F_G values of midazolam were estimated as 1.25 or 2.15-2.58 -fold, respectively (Supplemental Table S8).

Difference of pharmacokinetics of midazolam and digoxin in the fasted and fed states

It was considered that the drug behavior in the small intestine was different between the fasted and fed states from the analysis in Fig. 2. Therefore, using the

DMD Fast Forward. Published on May 7, 2021 as DOI: 10.1124/dmd.121.000361
This article has not been copyedited and formatted. The final version may differ from this version.

dispersion number and flow rate obtained in the analysis, the differences in plasma concentrations of midazolam or digoxin were compared between the fasted and fed states and evaluated their significance. As a result, both substrates exhibited decreased C_{max} and delayed t_{max} in the fed state (Fig. 9), showing tendencies consistent with the previous reports on the food effects on pharmacokinetics of midazolam and digoxin (Bornemann et al., 1986, Sanchez et al., 1973).

DMD Fast Forward. Published on May 7, 2021 as DOI: 10.1124/dmd.121.000361
This article has not been copyedited and formatted. The final version may differ from this version.

Discussion

Precise estimation of drug concentration in the enterocytes is indispensable to consider nonlinear drug absorption and DIs in which intestinal CYP3A and P-gp are involved. Accordingly, precise consideration of drug translocation in the intestinal lumen is necessary because the concentration in the lumen directly affects the concentration in enterocytes. Food intake affects bile secretion, pH, blood flow, and drug translocation in the intestine (Jantratid et al., 2008; Kawai et al., 2011; Fleisher et al., 1999) and often seriously modifies drug absorption with changes in its solubility in the lumen. Haruta et al. (2002) observed changes in drug translocation by monitoring the radioactivity of ^{99m}Tc-DTPA under the fasted and fed conditions. However, there have been few reports of absorption models to examine the precise drug translocation.

ATOM succeeded in reproducing the distribution of ^{99m}Tc-DTPA by applying a dispersion model with location-dependent dispersion number and time-dependent intestinal flow (Fig. 2 and 3). The behavior of drugs in the small intestine is quite complex because of its structure and varied motility (Sokolis, 2012). In fact, luminal ^{99m}Tc-DTPA movement was not simulated in models with fixed dispersion numbers and intestinal flow (Supplemental Fig. S2). In a preliminary analysis, we considered a model with location-dependent dispersion number and flow, but its reproducibility of

DMD Fast Forward. Published on May 7, 2021 as DOI: 10.1124/dmd.121.000361
This article has not been copyedited and formatted. The final version may differ from this version.

the drug movement under fed conditions was inferior to that of the adopted model. Therefore, time-dependent intestinal flow was also necessary to explain complex drug translocations in some cases.

Previously, GITA model explains luminal drug movements precisely using a set of first-order transit rates and lag-time (Sawamoto et al., 1997; Kimura and Higaki, 2002; Haruta et al., 2002). However, GITA model lacks the location-dependent physiological changes in the intestine, whereas CAT and ADAM considers them. In this study, however, CAT model could not reproduce luminal ^{99m}Tc-DTPA distribution, regardless of optimizing luminal transit times (Fig. 2E, F, G, H and Supplemental Fig. 2). For this reason, CAT appeared to overestimate $F_A F_G$ of midazolam at lower doses, whereas ATOM predicted the observed values satisfactorily (Fig. 6A). CYP3A expression level is higher in the upper intestine (Paine et al., 1997); thus, the retention of a drug in the upper intestine would be important for intestinal metabolism. CAT estimates a stronger saturation of CYP3A because of its higher concentration in the upper intestine compared with ATOM. The present study implies that intestinal absorption models that cannot explain intestinal translocation may lead to a misunderstanding of the nonlinear dynamics of drug absorption.

DMD Fast Forward. Published on May 7, 2021 as DOI: 10.1124/dmd.121.000361
This article has not been copyedited and formatted. The final version may differ from this version.

Intestinal DIs involving CYP3A or P-gp occur because of high drug concentration in the intestine after oral administration (Delavenne et al., 2013; Lilja et al., 2000). This is especially applicable for weak CYP3A inhibitors, since AUC increase of them mainly depends on intestinal DIs rather than hepatic ones where drug concentrations may be lower (Yamada et al., 2020). Several CYP3A and P-gp-mediated DIs have been analyzed using PBPK models (Yamazaki et al., 2019, Heikkinen et al., 2012); however, the appropriateness of drug concentrations in the small intestine was not discussed in detail. Currently, DI guidance for the US, Europe, and Japan only document one formula for estimation of intestinal drug concentration, which divides the dose by the amount of drinking water (250 mL). This is a useful approach for risk management, but far from the concept of PBPK analysis.

In this study, the significances of DIs for midazolam and digoxin cases were explained to a large extent by the intestinal contribution (Fig. 8), suggesting importance of the intestinal DIs. The DI between midazolam and itraconazole was extensively studied and contributions by the metabolites of itraconazole have been clarified (Isoherranen et al., 2004, Prieto Garcia et al., 2018, Chen et al., 2019) whereas the intestinal contribution was not fully evaluated. In this study, the contribution by the metabolites was not considered because their concentrations in the enterocytes are

DMD Fast Forward. Published on May 7, 2021 as DOI: 10.1124/dmd.121.000361
This article has not been copyedited and formatted. The final version may differ from this version.

unknown and would be lower than those in the liver. Nevertheless, in this study, ATOM somewhat overestimates the intestinal interaction by itraconazole. In the future, further detailed studies of DIs are necessary to conclude the precise interactions due to the intestinal contributions.

Regarding pharmacokinetics of digoxin, the contribution of P-gp may be not only in the intestine but potentially in the liver and kidney (Yin and Wang, 2016, Liu and Sahi, 2016). Therefore, DIs in the liver and kidney should also be considered, which was not achieved in this study. Nevertheless, the analysis of Fig. 8B demonstrated the significance of the intestinal contribution. On the other hand, the predictive performances of P-gp substrates such as cyclosporin and saquinavir were insufficient (Supplemental Table S6). It may be due to relatively high doses of these drugs, and thus causing saturation of P-gp. An extensive simulation study of P-gp substrates including verapamil, fexofenadine, talinolol as well as digoxin was performed by using TLM, and it was suggested that higher doses such as 100 mg, the risk of P-gp-mediated DI would generally be reduced because of saturation of P-gp efflux (Ando et al. 2015).

In addition to the luminal translocation issue, it is necessary to consider the permeability of the basolateral membrane to precisely estimate the drug concentration in

DMD Fast Forward. Published on May 7, 2021 as DOI: 10.1124/dmd.121.000361
This article has not been copyedited and formatted. The final version may differ from this version.

enterocytes. In the reported absorption models, ambiguity remains in the descriptions of the basolateral permeability because only one compartment is arranged for the portal blood along with the whole length of the small intestine. If permeation across the basolateral membrane were bidirectional, a drug would be back-secreted from the blood to the lower intestine immediately after absorption begins in the upper intestine. Since no one has reported this phenomenon, it can be assumed that permeation across the basolateral membrane is not truly bidirectional, implying that blood flow limited absorption cannot be considered by these models; even though the effect of blood flow on drug absorption has been discussed (Winne, 1978, Schulz and Winne, 1987; Chen and Pang, 1997; Pang and Chow, 2012). To solve this problem, the portal blood compartment needs to be separated conceptually by the location of the intestine as achieved in TLM and ATOM. Additionally, it is necessary to evaluate the permeability of the basolateral membrane separating from that of the apical membrane to incorporate these parameters into the model. This is still a challenging issue, but by using multifunctional cell systems such as induced pluripotent stem (iPS) cells (Kabeya et al., 2020) and CYP3A4-expressed intestinal cells (Takenaka et al., 2017), it may be possible to discriminate various kinetic intracellular events using selective inhibitors or knock-down techniques.

DMD Fast Forward. Published on May 7, 2021 as DOI: 10.1124/dmd.121.000361
This article has not been copyedited and formatted. The final version may differ from this version.

To precisely reproduce *in vivo* situations, PBPK model is composed of complicated structures and parameters, including multiple scaling factors for filling gaps between *in vitro* and *in vivo* studies. However, in the case of the intestinal absorption model, if the scaling factor is used to adjust for ambiguity of the absorption site, it should lose its validity for drugs with different absorption sites. In other words, the role of scaling factors is to adjust simply quantitative relationships between *in vitro* and *in vivo*. Regarding CYP3A and P-gp substrates, Takano et al. (2016) reported a non-linear prediction of pharmacokinetics of midazolam successfully with a scaling factor for V_{max} of CYP3A and explained dose-dependent F_AF_G. However, the appropriateness of the scaling factor was not discussed. In this study, the nonlinear absorption of midazolam was predicted using ATOM minimized to only the scaling factors of passive permeability and P-gp expression (Fig. 6A and Supplementary text). Therefore, we expect that analysis using ATOM would be a useful approach for predicting pharmacokinetics in multiple situations including drug development.

Theoretically, the predicted clearance of an organ pharmacokinetic model is determined by the residence time distribution of the solute and the clearance in the organ (Roberts et al., 1988). ATOM and TLM are designed to be equivalent for these values, so there should be no difference in prediction performance. The performances of

DMD Fast Forward. Published on May 7, 2021 as DOI: 10.1124/dmd.121.000361
This article has not been copyedited and formatted. The final version may differ from this version.

ATOM and TLM are comparable to other sophisticated models such as ACAT (Ando et al., 2015, Gertz et al., 2010, Yau et al., 2017). However, their superiority has not been proved yet. Currently, some *in vitro* parameters for predicting oral availability including the transport activity by P-gp (Bentz et al., 2013) are variable between experiments and reliable *in vivo* F_A and F_G values are insufficient (Hisaka et al., 2014). Therefore, further studies are necessary to select the better absorption model.

In the process of drug absorption, dissociation and dissolution are also regulating factors, especially for highly lipophilic and potentially insoluble compounds. These factors are readily influenced by luminal pH, which is lower in the stomach (pH: 1.5-5.0), but gradually increases in the intestine (pH: 5.0-7.4) (DeSesso and Williams, 2008). At present, ATOM does not include these processes and only considers drug aqueous solutions. Therefore, it is necessary to expand ATOM by incorporating these processes to broaden its applicability.

In conclusion, a newly constructed absorption model, ATOM, could simulate intestinal drug behavior using minimum scaling factors, thereby providing reasonable interpretations of change in drug absorption and of DI mediated by CYP3A and P-gp. In the future, ATOM is expected to be applied to drug development and clinical management.

DMD Fast Forward. Published on May 7, 2021 as DOI: 10.1124/dmd.121.000361
This article has not been copyedited and formatted. The final version may differ from this version.

Acknowledgements

The authors thank Teijin Pharma Limited for their assistance. This work was supported by AMED under Grant Number JP20be0304203 and by the Basis for Supporting Innovative Drug Discovery and Life Science Research (BINDS) from AMED under grant number JP20am0101124 (YK).

DMD Fast Forward. Published on May 7, 2021 as DOI: 10.1124/dmd.121.000361
This article has not been copyedited and formatted. The final version may differ from this version.

Authorship Contributions

Participated in research design: Asano, Sato, Hisaka.

Conducted experiments: Asano, Yoshitomo

Contributed new reagents or analytic tools: Asano, Hozuki, Hisaka.

Performed data analysis: Asano, Hisaka.

Wrote or contributed to the writing of the manuscript: Asano, Sato, Kazuki, Hisaka.

DMD Fast Forward. Published on May 7, 2021 as DOI: 10.1124/dmd.121.000361
This article has not been copyedited and formatted. The final version may differ from this version.

References

Agoram B, Woltosz WS, Bolger MB (2001) Predicting the impact of physiological and biochemical processes on oral drug bioavailability. *Adv Drug Deliv Rev*. **50** Suppl 1:S41-S67.

Ando H, Hisaka A, Suzuki H (2015) A new physiologically based pharmacokinetic model for the prediction of gastrointestinal drug absorption: translocation model. *Drug Metab Dispos*. **43**(4):590-602.

Ando H, Hatakeyama H, Sato H, Hisaka A, Suzuki H (2017) Determinants of Intestinal Availability for P-glycoprotein Substrate Drugs Estimated by Extensive Simulation With Mathematical Absorption Models. *J Pharm Sci*. **106**(9):2771-2779.

Bolger MB, Lukacova V, Woltosz WS (2009) Simulations of the nonlinear dose dependence for substrates of influx and efflux transporters in the human intestine. *AAPS J*. **11**(2):353-363.

Bentz J, O'Connor MP, Bednarczyk D, Coleman J, Lee C, Palm J, Pak YA, Perloff ES, Reyner E, Balimane P, Brännström M, Chu X, Funk C, Guo A, Hanna I, Herédi-Szabó K, Hillgren K, Li L, Hollnack-Pusch E, Jamei M, Lin X, Mason AK, Neuhoff S, Patel A, Podila L, Plise E, Rajaraman G, Salphati L, Sands E, Taub ME, Taur JS, Weitz D, Wortelboer HM, Xia CQ, Xiao G, Yabut J, Yamagata T, Zhang L, Ellens H (2013) Variability in P-glycoprotein inhibitory potency (IC_{50}) using various in vitro experimental systems: implications for universal digoxin drug-drug interaction risk assessment decision criteria. *Drug Metab Dispos*. **41**(7):1347-1366.

Bornemann LD, Crews T, Chen SS, Twardak S, Patel IH (1986) Influence of food on midazolam absorption. *J Clin Pharmacol*. **26**(1):55-59.

Chen J, Pang KS (1997) Effect of flow on first-pass metabolism of drugs: single pass studies on 4-methylumbelliferone conjugation in the serially perfused rat intestine and liver preparations. *J Pharmacol Exp Ther*. **280**(1):24-31.

Chen Y, Cabalu TD, Callegari E, Einolf H, Liu L, Parrott N, Peters SA, Schuck E, Sharma P, Tracey H, Upreti VV, Zheng M, Zhu AZX, Hall SD (2019)

Recommendations for the Design of Clinical Drug-Drug Interaction Studies With Itraconazole Using a Mechanistic Physiologically-Based Pharmacokinetic Model. *CPT Pharmacometrics Syst Pharmacol*. **8**(9):685-695.

Chu X, Galetin A, Zamek-Gliszczynski MJ, Zhang L, Tweedie DJ, International Transporter Consortium (2018) Dabigatran Etexilate and Digoxin: Comparison as Clinical Probe Substrates for Evaluation of P-gp Inhibition. *Clin Pharmacol Ther*. **104**(5):788-792.

Cong D, Doherty M, Pang KS (2000) A new physiologically based, segregated-flow model to explain route-dependent intestinal metabolism. *Drug Metab Dispos*. **28**(2):224-235.

Delavenne X, Ollier E, Basset T, Bertoletti L, Accassat S, Garcin A, Laporte S, Zufferey P, Mismetti P (2013) A semi-mechanistic absorption model to evaluate drug-drug interaction with dabigatran: application with clarithromycin. *Br J Clin Pharmacol*. **76**(1):107-113.

DeSesso JM, Williams AL (2008) Contrasting the Gastrointestinal Tracts of Mammals: Factors that Influence Absorption. *Annu Rep Med Chem*. **43**: 353-371.

Fleisher D, Li C, Zhou Y, Pao LH, Karim A (1999) Drug, meal and formulation interactions influencing drug absorption after oral administration. Clinical implications. *Clin Pharmacokinet*. **36**(3):233-254.

Galetin A, Gertz M, Houston JB (2010) Contribution of intestinal cytochrome p450-mediated metabolism to drug-drug inhibition and induction interactions. *Drug Metab Pharmacokinet*. **25**(1):28-47.

Gertz M, Harrison A, Houston JB, Galetin A (2010) Prediction of human intestinal first-pass metabolism of 25 CYP3A substrates from in vitro clearance and permeability data. *Drug Metab Dispos*. **38**(7):1147-1158.

Haruta S, Kawai K, Nishii R, Jinnouchi S, Ogawara Ki, Higaki K, Tamura S, Arimori K, Kimura T (2002) Prediction of plasma concentration-time curve of orally administered

theophylline based on a scintigraphic monitoring of gastrointestinal transit in human volunteers. *Int J Pharm*. **21**;233(1-2):179-190.

Heikkinen AT, Baneyx G, Caruso A, Parrott N (2012) Application of PBPK modeling to predict human intestinal metabolism of CYP3A substrates - an evaluation and case study using GastroPlus. *Eur J Pharm Sci*. **47**(2):375-386.

Hendriksen BA, Felix MV, Bolger MB (2003) The composite solubility versus pH profile and its role in intestinal absorption prediction. *AAPS PharmSci*. **5**(1):E4

Hisaka A, Nakamura M, Tsukihashi A, Koh S, Suzuki H (2014) Assessment of intestinal availability (FG) of substrate drugs of cytochrome p450s by analyzing changes in pharmacokinetic properties caused by drug-drug interactions. *Drug Metab Dispos*. **42**(10):1640-1645.

Hisaka A, Sugiyama Y (1998) Analysis of nonlinear and nonsteady state hepatic extraction with the dispersion model using the finite difference method. *J Pharmacokinet Biopharm*. **26**(5):495-519.

Homayun B, Lin X, Choi HJ (2019) Challenges and Recent Progress in Oral Drug Delivery Systems for Biopharmaceuticals. *Pharmaceutics*. **11**(3):129.

Huang W, Lee SL, Yu LX (2009) Mechanistic approaches to predicting oral drug absorption. *AAPS J*. **11**(2):217-224.

Isoherranen N, Kunze KL, Allen KE, Nelson WL, Thummel KE (2004) Role of itraconazole metabolites in CYP3A4 inhibition. *Drug Metab Dispos*. **32**(10):1121-1131.

Jamei M, Turner D, Yang J, Neuhoff S, Polak S, Rostami-Hodjegan A, Tucker G (2009) Population-based mechanistic prediction of oral drug absorption. *AAPS J*. **11**(2):225-237.

Jantratid E, Janssen N, Reppas C, Dressman JB (2008) Dissolution media simulating conditions in the proximal human gastrointestinal tract: an update. *Pharm Res*. **25**(7):1663-1676.

Kabeya T, Mima S, Imakura Y, Miyashita T, Ogura I, Yamada T, Yasujima T, Yuasa H, Iwao T, Matsunaga T (2020) Pharmacokinetic functions of human induced pluripotent stem cell-derived small intestinal epithelial cells. *Drug Metab Pharmacokinet*. **35**(4):374-382.

Kawai Y, Fujii Y, Tabata F, Ito J, Metsugi Y, Kameda A, Akimoto K, Takahashi M (2011) Profiling and trend analysis of food effects on oral drug absorption considering micelle interaction and solubilization by bile micelles. *Drug Metab Pharmacokinet*. **26**(2):180-191.

Kharasch ED, Walker A, Hoffer C, Sheffels P (2004) Intravenous and oral alfentanil as in vivo probes for hepatic and first-pass cytochrome P450 3A activity: noninvasive assessment by use of pupillary miosis. *Clin Pharmacol Ther*. **76**(5):452-466.

Kimura T, Higaki K (2002) Gastrointestinal transit and drug absorption. *Biol Pharm Bull.* **25**(2):149-164.

Lilja JJ, Kivistö KT, Neuvonen PJ (2000) Duration of effect of grapefruit juice on the pharmacokinetics of the CYP3A4 substrate simvastatin. *Clin Pharmacol Ther*. **68**(4):384-390.

Liu H, Sahi J (2016) Role of Hepatic Drug Transporters in Drug Development. *J Clin Pharmacol*. **56** Suppl 7:S11-22.

Lu J, Shao Y, Qin X, Liu D, Chen A, Li D, Liu M, Wang X (2017) CRISPR knockout rat cytochrome P450 3A1/2 model for advancing drug metabolism and pharmacokinetics research. *Sci Rep.* **20**;7:42922.

Matheson PJ, Wilson MA, Garrison RN (2000) Regulation of intestinal blood flow. *J Surg Res*. **93**(1):182-196.

Mayer U, Wagenaar E, Beijnen JH, Smit JW, Meijer DK, van Asperen J, Borst P, Schinkel AH (1996) Substantial excretion of digoxin via the intestinal mucosa and prevention of long-term digoxin accumulation in the brain by the mdr 1a P-glycoprotein. *Br J Pharmacol.* **119**(5):1038-1044.

Mudie DM, Murray K, Hoad CL, Pritchard SE, Garnett MC, Amidon GL, Gowland PA, Spiller RC, Amidon GE, Marciani L (2014) Quantification of gastrointestinal liquid volumes and distribution following a 240 mL dose of water in the fasted state. *Mol Pharm*. **11**(9):3039-3047.

Paine MF, Khalighi M, Fisher JM, Shen DD, Kunze KL, Marsh CL, Perkins JD, Thummel KE (1997) Characterization of interintestinal and intraintestinal variations in human CYP3A-dependent metabolism. *J Pharmacol Exp Ther*. **283**(3):1552-1562.

Pang KS, Chow EC (2012) Commentary: theoretical predictions of flow effects on intestinal and systemic availability in physiologically based pharmacokinetic intestine models: the traditional model, segregated flow model, and QGut model. *Drug Metab Dispos*. **40**(10):1869-1877.

Poulin P, Jones RD, Jones HM, Gibson CR, Rowland M, Chien JY, Ring BJ, Adkison KK, Ku MS, He H, Vuppugalla R, Marathe P, Fischer V, Dutta S, Sinha VK, Björnsson T, Lavé T, Yates JW (2011) PHRMA CPCDC initiative on predictive models of human

pharmacokinetics, part 5: prediction of plasma concentration-time profiles in human by using the physiologically-based pharmacokinetic modeling approach. *J Pharm Sci*. **100**(10):4127-4157.

Prieto Garcia L, Janzén D, Kanebratt KP, Ericsson H, Lennernäs H, Lundahl A (2018) Physiologically Based Pharmacokinetic Model of Itraconazole and Two of Its Metabolites to Improve the Predictions and the Mechanistic Understanding of CYP3A4 Drug-Drug Interactions. *Drug Metab Dispos.* **46**(10):1420-1433.

Rengelshausen J, Göggelmann C, Burhenne J, Riedel KD, Ludwig J, Weiss J, Mikus G, Walter-Sack I, Haefeli WE (2003) Contribution of increased oral bioavailability and reduced nonglomerular renal clearance of digoxin to the digoxin-clarithromycin interaction. *Br J Clin Pharmacol*. **56**(1):32-38.

Roberts MS, Donaldson JD, Rowland M (1988) Models of hepatic elimination: comparison of stochastic models to describe residence time distributions and to predict the influence of drug distribution, enzyme heterogeneity, and systemic recycling on hepatic elimination. *J Pharmacokinet Biopharm*. **16**(1):41-83.

Roberts MS, Rowland M (1986) A dispersion model of hepatic elimination: 1. Formulation of the model and bolus considerations. *J Pharmacokinet Biopharm*. **14**(3):227-260.

Rostami-Hodjegan A, Tucker G (2004) 'In silico' simulations to assess the 'in vivo' consequences of 'in vitro' metabolic drug-drug interactions. *Drug Discov Today Technol.* **1**(4):441-448.

Sanchez N, Sheiner LB, Halkin H, Melmon KL (1973) Pharmacokinetics of digoxin: interpreting bioavailability. *Br Med J.* **4**(5885):132-134.

Schulz R, Winne D (1987) Relationship between antipyrine absorption and blood flow rate in rat jejunum, ileum, and colon. *Naunyn Schmiedebergs Arch Pharmacol.* **335**(1):97–102.

Sokolis DP (2017) Experimental study and biomechanical characterization for the passive small intestine: Identification of regional differences. *J Mech Behav Biomed Mater*. **74**:93-105.

Takenaka T, Kazuki K, Harada N, Kuze J, Chiba M, Iwao T, Matsunaga T, Abe S, Oshimura M, Kazuki Y (2017) Development of Caco-2 cells co-expressing CYP3A4 and NADPH-cytochrome P450 reductase using a human artificial chromosome for the prediction of intestinal extraction ratio of CYP3A4 substrates. *Drug Metab Pharmacokinet*. **32**(1):61-68.

Takano J, Maeda K, Bolger MB, Sugiyama Y (2016) The Prediction of the Relative Importance of CYP3A/P-glycoprotein to the Nonlinear Intestinal Absorption of Drugs by Advanced Compartmental Absorption and Transit Model. *Drug Metab Dispos*. **44**(11):1808-1818.

Templeton I, Peng CC, Thummel KE, Davis C, Kunze KL, Isoherranen N (2010) Accurate prediction of dose-dependent CYP3A4 inhibition by itraconazole and its metabolites from in vitro inhibition data. *Clin Pharmacol Ther*. **88**(4):499-505.

von Richter O, Burk O, Fromm MF, Thon KP, Eichelbaum M, Kivistö KT (2004) Cytochrome P450 3A4 and P-glycoprotein expression in human small intestinal enterocytes and hepatocytes: a comparative analysis in paired tissue specimens. *Clin Pharmacol Ther*. **75**(3):172-183.

Winne D (1978) Blood flow in intestinal absorption models. *J Pharmacokinet Biopharm*. **6**(1):55-78.

Yamada M, Inoue SI, Sugiyama D, Nishiya Y, Ishizuka T, Watanabe A, Watanabe K, Yamashita S, Watanabe N (2020) Critical Impact of Drug-Drug Interactions via Intestinal CYP3A in the Risk Assessment of Weak Perpetrators Using Physiologically Based Pharmacokinetic Models. *Drug Metab Dispos*. **48**(4):288-296.

Yamazaki S, Costales C, Lazzaro S, Eatemadpour S, Kimoto E, Varma MV (2019) Physiologically-Based Pharmacokinetic Modeling Approach to Predict Rifampin-Mediated Intestinal P-Glycoprotein Induction. *CPT Pharmacometrics Syst Pharmacol.* **8**(9):634-642.

Yau E, Petersson C, Dolgos H, Peters SA (2017) A comparative evaluation of models to predict human intestinal metabolism from nonclinical data. *Biopharm Drug Dispos*. **38**(3):163-186.

Yin J, Wang J (2016) Renal drug transporters and their significance in drug-drug interactions. *Acta Pharm Sin B*. **6**(5):363-373.

Yu LX, Amidon GL (1999) A compartmental absorption and transit model for estimating oral drug absorption. *Int J Pharm*. **186**(2):119-125

DMD Fast Forward. Published on May 7, 2021 as DOI: 10.1124/dmd.121.000361
This article has not been copyedited and formatted. The final version may differ from this version.

Footnotes

Satoshi Asano is affiliated with Teijin Pharma Limited and this study was partly supported by Teijin Pharma Limited. However, Teijin Pharma Limited was not involved in the planning and analysis of this study. No author has an actual or perceived conflict of interest with the contents of this article.

DMD Fast Forward. Published on May 7, 2021 as DOI: 10.1124/dmd.121.000361
This article has not been copyedited and formatted. The final version may differ from this version.

Figure legends

Fig. 1 Structures of ATOM (A) and CAT model (B).

Parameter z shows the normalized length from the inlet of the small intestine, which is equal to the ratio of intestinal volume until the location to the full volume. Descriptions of parameters in these models are shown in Table 1.

Fig. 2 Simulated movements of ^{99m}Tc-DTPA in the gastrointestinal tract by ATOM (A, B, C and D) and CAT (E, F, G and H) in fasted and fed state.

The observed ^{99m}Tc-DTPA distribution in the lumen was taken from a previous study (Haruta et al., 2002), which reported its distribution in two subjects. Simulated results of ^{99m}Tc-DTPA distribution of subject A in the fasted condition (A and E), subject A in the fed condition (B and F), subject B in the fasted condition (C and G), and subject B in the fed condition (D and H). The left (A, B, C and D) and right (E, F, G and H) panels show the simulated results by ATOM and CAT, respectively. Open circles, closed circles, open squares, and open triangles represent the observed distributions in the stomach, upper intestine, lower intestine, and caecum/colon, respectively. The lines represent the simulated ^{99m}Tc-DTPA distributions in each organ. In ATOM, distributions at 40 locations were simulated, and the upper 24 segments were assigned

DMD Fast Forward. Published on May 7, 2021 as DOI: 10.1124/dmd.121.000361
This article has not been copyedited and formatted. The final version may differ from this version.

to the upper intestine and the other 16 segments to the lower intestine corresponding to CAT model using the index of the length from the inlet in the intestine. CAT model assumes that the small intestine is divided into six portions, as shown in Fig. 1.

Fig. 3 Optimized change of location-dispersion number (A and B) and time-dependent flow rates (C and D) in the small intestine in ATOM.

Each dispersion number and flow rate were obtained by optimization using the observed ^{99m}Tc-DTPA distribution reported by Haruta et al. (2002), as shown in Fig. 2. Solid and dotted lines represent the obtained profiles of the dispersion number or flow rate using ^{99m}Tc-DTPA distribution of subject A and subject B, respectively. Panels A and C show the obtained dispersion numbers and flow rates in the fasted condition, while panels B and D represent those in the fed condition. The equations for calculating the location-dependent dispersion number and time-dependent flow rate are shown in the Method.

Fig. 4 Demonstrative simulation using ATOM and CAT model of drug concentrations in enterocytes in the small intestine at 0.5 h (A), 2 h (B) and 6 h (C) after oral administration.

DMD Fast Forward. Published on May 7, 2021 as DOI: 10.1124/dmd.121.000361
This article has not been copyedited and formatted. The final version may differ from this version.

Solid and broken lines show simulated results by ATOM and CAT model with optimized transit times, respectively. The model compound has the same physiological and pharmacokinetic parameters (molecular weight, pKa values, $K_{m,CYP3A}$, and unbound fractions in plasma, blood and enterocytes) as midazolam, except for its apparent permeability in Caco-2 cells ($P_{app,Caco-2}$) and $V_{max,CYP3A}$, set as 0.002 cm/h (approximately 1/50 compared with midazolam) and 0 μg /h pmol CYP3A, respectively. The dispersion number and flow rate in the intestine obtained in the analysis shown in Fig. 2A using ^{99m}Tc-DTPA distribution of subject A in the fasted state as reported by Haruta et al. (2002) were adapted. Dose was set to 1 ng.

Fig. 5 Demonstrative simulation of cumulative drug absorption by ATOM and CAT model.

Solid and broken lines represent cumulative drug transfer into the portal vein simulated by ATOM and CAT with optimized transit times, respectively. The simulation was performed using the same model drug, which was absorbed only by passive diffusion with low permeability, as shown in Fig. 4. The dispersion number and flow rate in the intestine obtained in the analysis shown in Fig. 2A using ^{99m}Tc-DTPA distribution of

DMD Fast Forward. Published on May 7, 2021 as DOI: 10.1124/dmd.121.000361
This article has not been copyedited and formatted. The final version may differ from this version.

subject A in the fasted state as reported by Haruta et al. (2002) were adapted. Dose was set to 1 ng.

Fig. 6 Simulation of dose-dependent F_AF_G change of midazolam (A) and comparison of simulated unbound drug concentration in enterocytes between ATOM and CAT with optimized transit times (B) in fasted and fed state.

In panel A, closed circles represent reported F_AF_G values according to previous reports (Ando et al., 2015; Bornemann et al., 1985). Black bold, black dotted, and blue bold lines represent the predicted dose-dependent F_AF_G profiles of midazolam by ATOM in fasted state, by CAT in fasted state, and by ATOM in fed state, respectively.

In panel B, the maximum unbound concentration in enterocytes was reached in two models at 0.16 h after oral administration. Black bold, black dotted, and blue bold lines represent the predicted unbound concentration of midazolam in enterocytes by ATOM in fasted state, by CAT in fasted state, and by ATOM in fed state, respectively. The red line represents $K_{m,CYP3A,u}$ of midazolam (1.08 μg/mL), as reported previously (Ando et al., 2015). In this analysis, the dispersion number and flow rate in the intestine obtained in the analysis shown in Fig. 2A using ^{99m}Tc-DTPA distribution of subject A in the fasted state as reported by Haruta et al. (2002) were adapted.

DMD Fast Forward. Published on May 7, 2021 as DOI: 10.1124/dmd.121.000361
This article has not been copyedited and formatted. The final version may differ from this version.

Fig. 7 Comparison of F_G values using ATOM and TLM.

F_G values of 17 CYP3A or CYP3A/P-gp substrates (alfentanil, alprazolam, buspirone, cisapride, cyclosporin, felodipine, lovastatin, midazolam, nifedipine, nisoldipine, rifabutin, saquinavir, sildenafil, simvastatin, trazodone, triazolam, and zolpidem) were evaluated using ATOM. The dotted and solid lines represent 100 % and 90 - 110 % of the predicted F_G values obtained using TLM, respectively. F_G values predicted by TLM were obtained from a previous report by Ando et al. (2015).

Fig. 8 Demonstrative simulation of CYP3A (A) or P-gp (B) mediated-DI using ATOM.

In panel A, open circles, closed circles, open squares, and open triangles represent the concentration of midazolam in plasma with 0, 50, 200, and 400 mg itraconazole, respectively. The observed plasma concentrations of midazolam by Templeton et al. (2010) were used in the simulation. Itraconazole was administered once daily at 50, 200, or 400 mg during the study (from t = 0 h). Midazolam was administered 4 h after the administration of itraconazole.

In panel B, open and closed circles represent the plasma concentration of digoxin with 0 and 250 mg clarithromycin twice daily. Observed plasma concentrations of digoxin by

DMD Fast Forward. Published on May 7, 2021 as DOI: 10.1124/dmd.121.000361
This article has not been copyedited and formatted. The final version may differ from this version.

Rengelshausen et al. (2003) were used in the simulation. Clarithromycin was administered twice daily (250 mg each) during the study period (from t = 0 h). Digoxin was administered 24 h after the first administration of clarithromycin. In both analyses, the dispersion number and flow rate in the intestine obtained in the analysis shown in Fig. 2A using ^{99m}Tc-DTPA distribution of subject A in the fasted state reported by Haruta et al. (2002) were adapted. The symbols and error bars represent the mean concentration in plasma and SD, respectively.

Fig. 9 Plasma concentration of midazolam (A) and digoxin (B) after oral administration in fasted and fed state.

Solid and broken line represent the plasma concentration profile of midazolam (A) or digoxin (B) in fasted and fed state, respectively. Doses were set to 2 mg (midazolam) or 0.75 mg (digoxin). The dispersion number and flow rate in the intestine obtained in the analysis shown in Fig. 2A and 2B using ^{99m}Tc-DTPA distribution of subject A in the fasted and fed state as reported by Haruta et al. (2002) were adopted. Predicted C_{max} values of midazolam in fasted and fed state were 0.0225 and 0.0164 μmol/L, and those of digoxin in fasted and fed state were 3.51 and 1.51 ng/mL, respectively. Predicted t_{max}

DMD Fast Forward. Published on May 7, 2021 as DOI: 10.1124/dmd.121.000361
This article has not been copyedited and formatted. The final version may differ from this version.

values of midazolam in fasted and fed state were 0.86 and 1.35 h, and those of digoxin in fasted and fed state were 0.96 and 1.20 h, respectively.

DMD Fast Forward. Published on May 7, 2021 as DOI: 10.1124/dmd.121.000361
This article has not been copyedited and formatted. The final version may differ from this version.

Table 1 Descriptions of parameters in ATOM and CAT

Parameters	Description
CL_{ent}	intestinal metabolic clearance by CYP3A
CL_{int}	hepatic intrinsic clearance
CL_R	renal clearance
D_z	location-dependent dispersion number
f_h	hepatic unbound fraction
k_{col}	transit rate from the ileum to the caecum/colon
k_{es}	transit rate of drug from the esophagus to the stomach
k_{feces}	transit rate from the caecum/colon to the feces
k_{n1}	transit rate from the nth peripheral compartment to the central compartment
k_{sto}	transit rate of drug from the stomach to the jejunum
$k_{t,n}$	transit rate from the nth compartment in the small intestine in CAT
k_{1n}	transit rate from the central compartment to the nth peripheral compartment
M_t	time-dependent intestinal flow rate

DMD Fast Forward. Published on May 7, 2021 as DOI: 10.1124/dmd.121.000361
This article has not been copyedited and formatted. The final version may differ from this version.

$PS_{a,in}$	permeability clearance from the lumen to the enterocytes in the apical membrane
$PS_{a,out}$	permeability clearance from the enterocytes to the lumen in the apical membrane
$PS_{b,in}$	permeability clearance from the enterocytes to the lamina propria in the basolateral membrane
$PS_{b,out}$	permeability clearance from the lamina propria to the enterocytes in the basolateral membrane
PS_{ent}	overall clearance in the basolateral membrane
Q_h	blood flow in the liver
Q_{ha}	arterial blood flow in the liver
Q_{pro}	blood flow rate in the lamina propria
Q_{pv}	blood flow rate in the portal vein

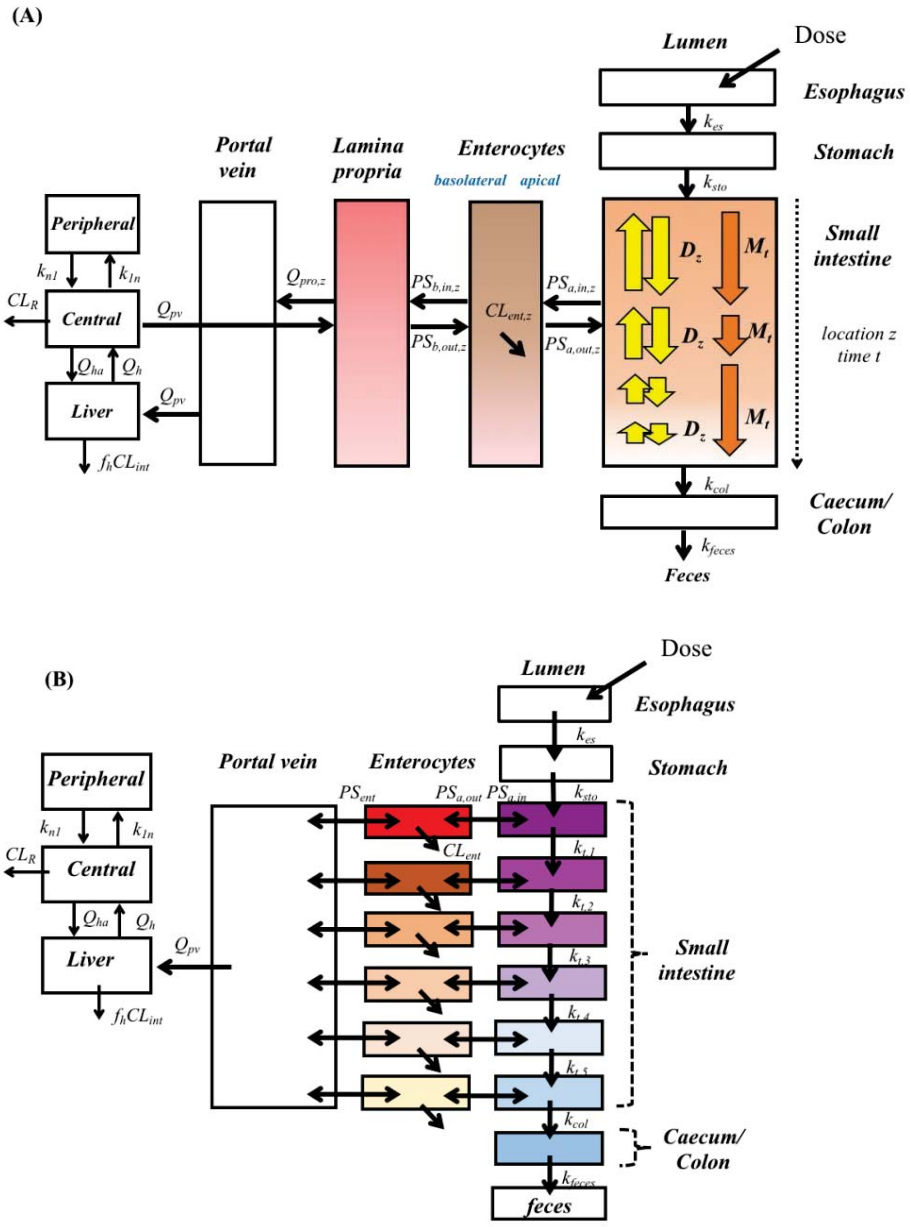

Fig. 1

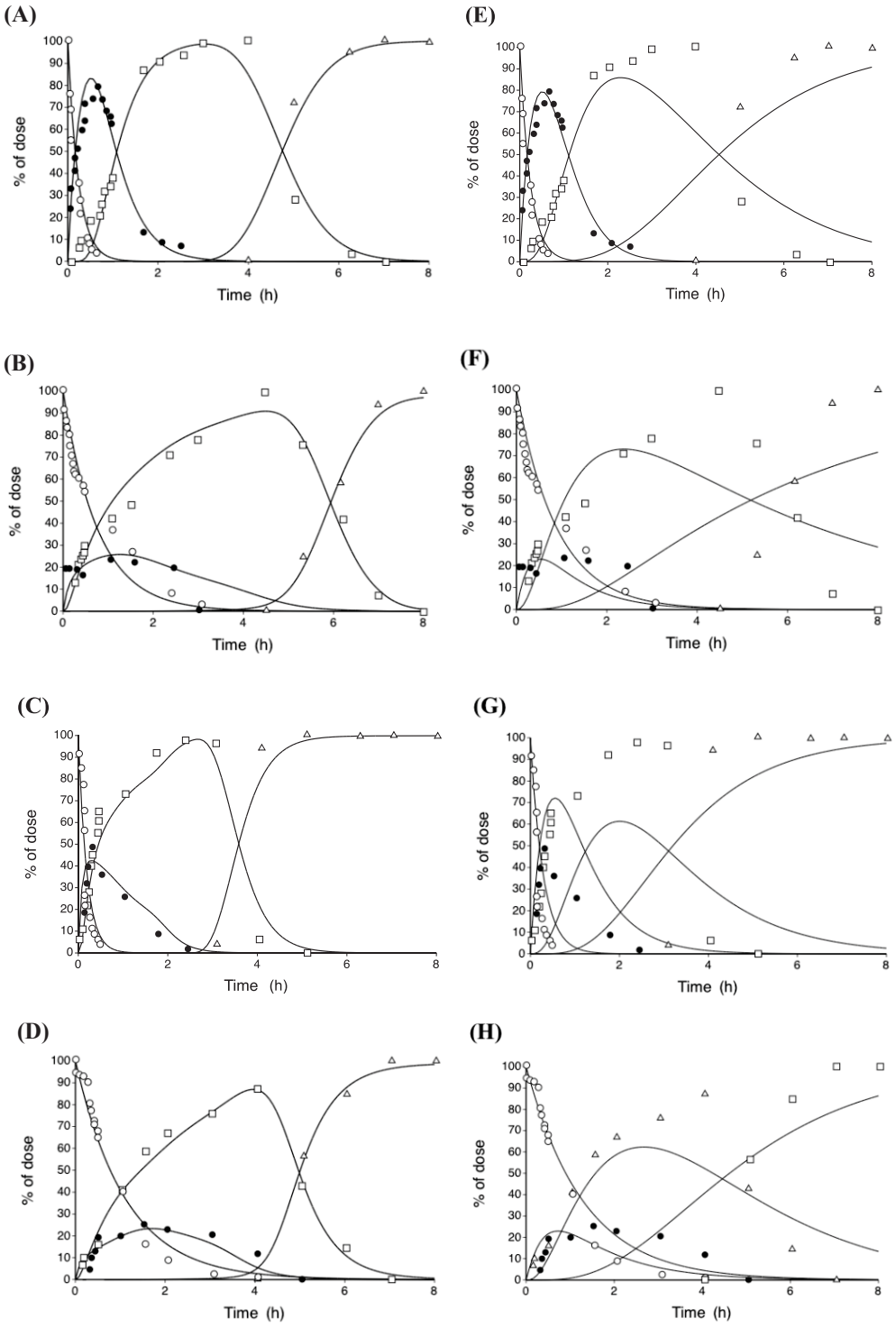

Fig. 2

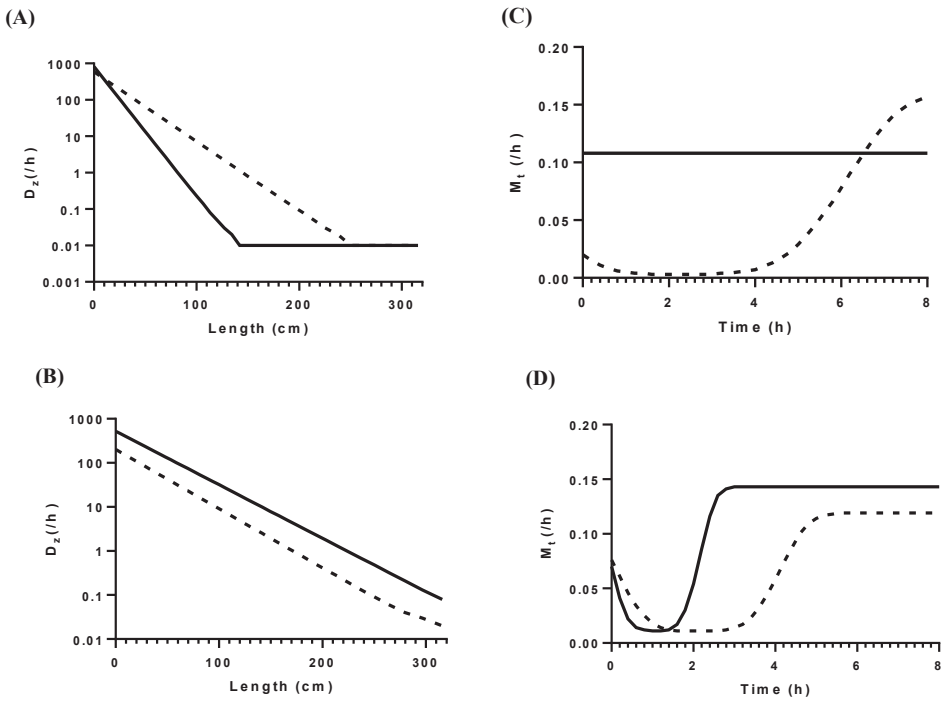

Fig. 3

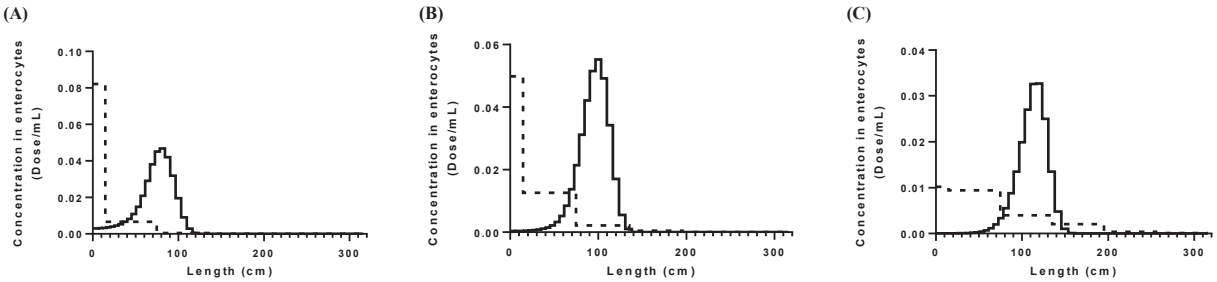

Fig. 4

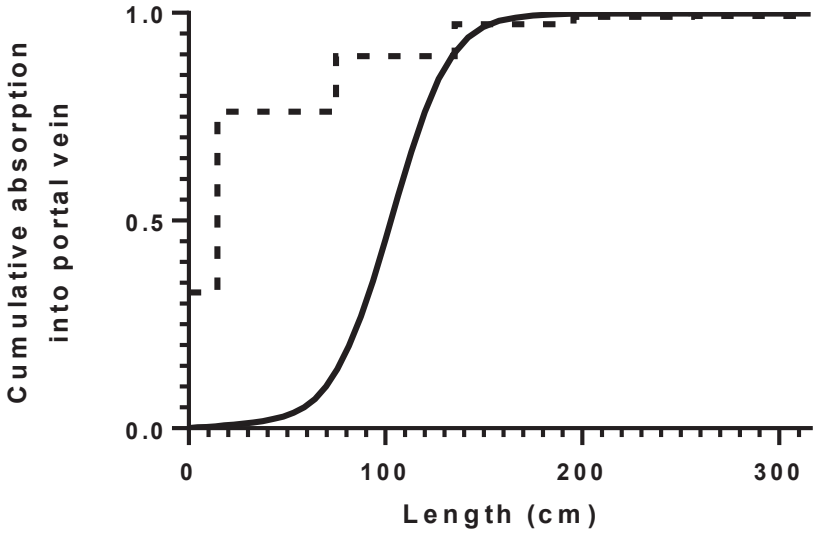

Fig. 5

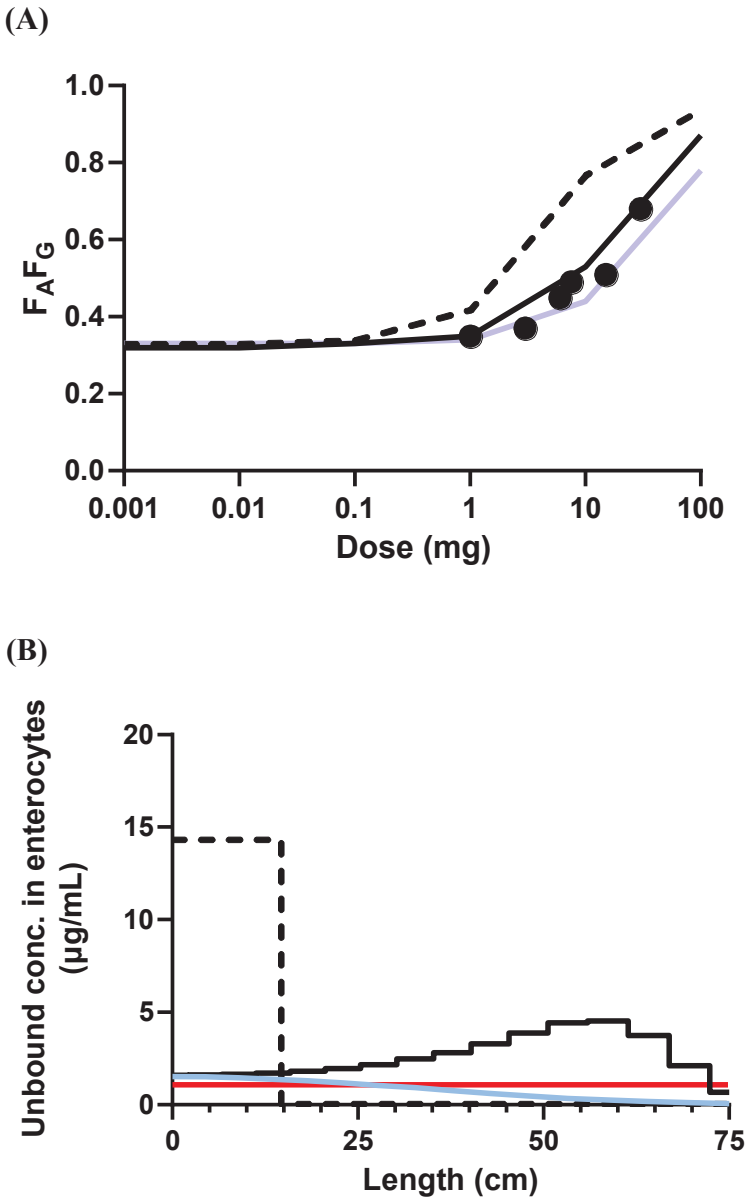

Fig. 6

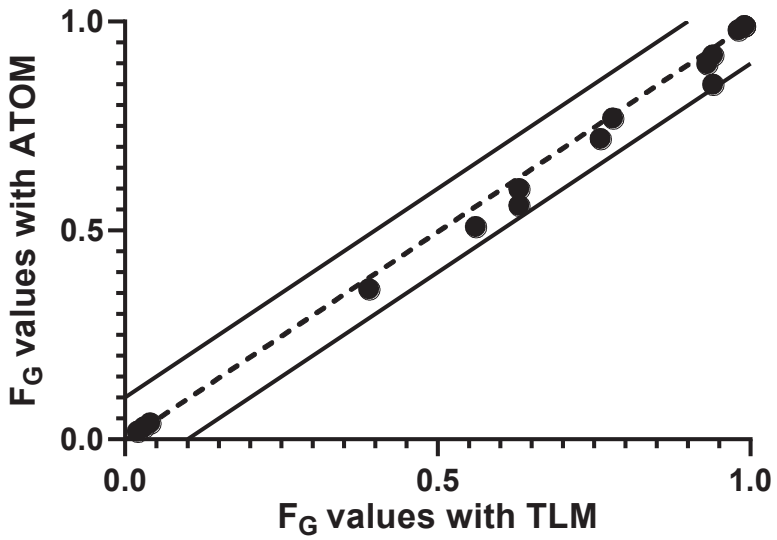

Fig. 7

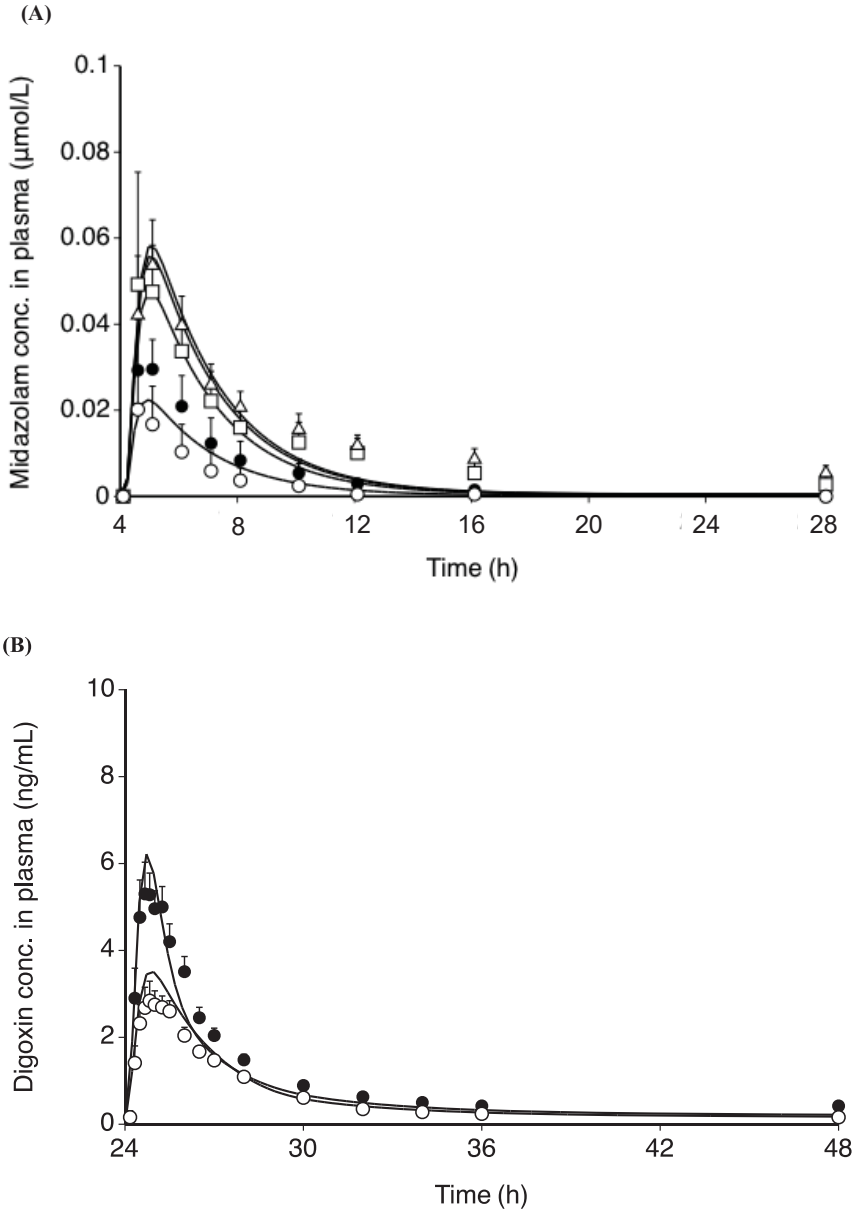

Fig. 8

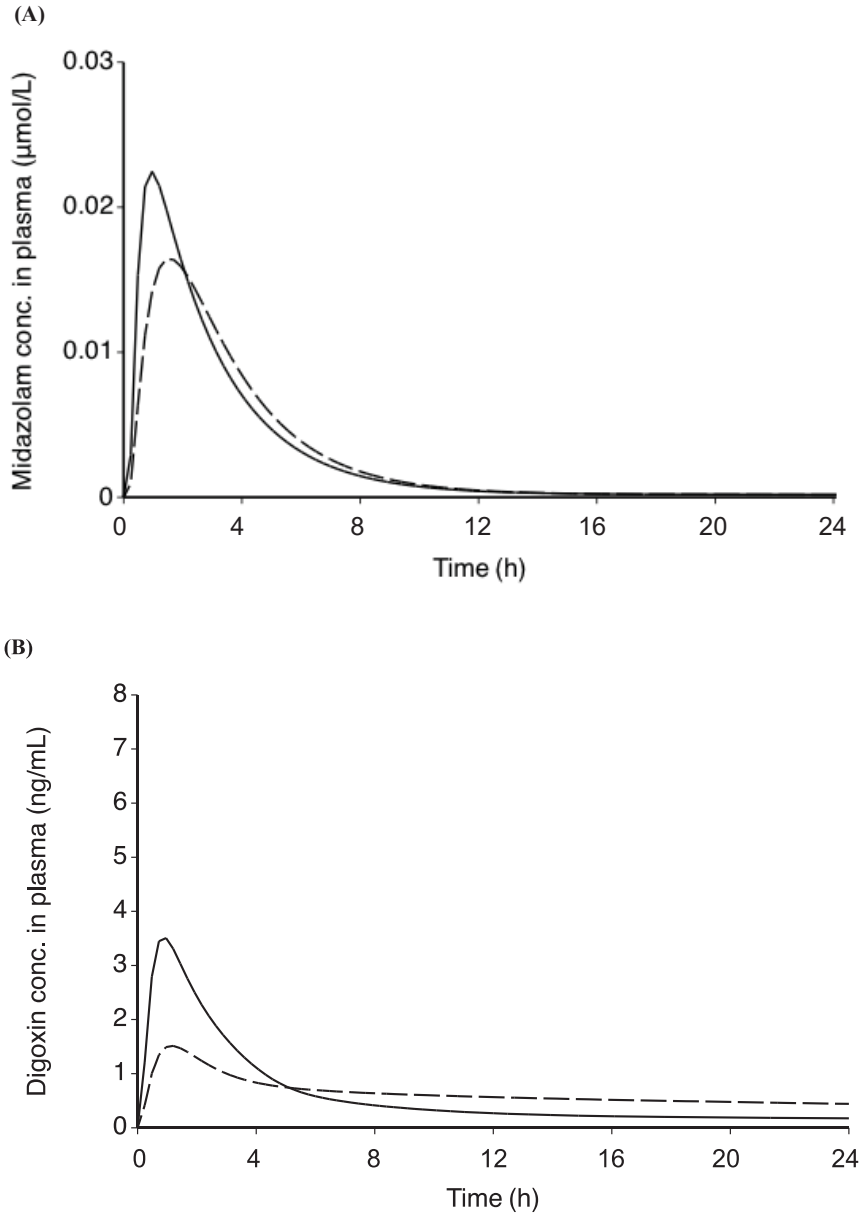

Fig. 9